Spontaneous Polarization and Bulk Photovoltaic Effect Driven by Polar Discontinuity in $LaFeO_3/SrTiO_3$ Heterojunctions

M. Nakamura,[1,*] F. Kagawa,[1] T. Tanigaki,[1,†] H. S. Park,[1,‡] T. Matsuda,[2] D. Shindo,[1,3] Y. Tokura,[1,4] and M. Kawasaki[1,4]
[1]*RIKEN Center for Emergent Matter Science (CEMS), Wako 351-0198, Japan*
[2]*Japan Science and Technology Agency (JST), Kawaguchi 332-0012, Japan*
[3]*Institute of Multidisciplinary Research for Advanced Materials, Tohoku University, Sendai 980-8577, Japan*
[4]*Department of Applied Physics and Quantum Phase Electronics Center (QPEC), University of Tokyo, Tokyo 113-8656, Japan*
(Received 27 November 2015; revised manuscript received 7 March 2016; published 11 April 2016)

Structurally coherent and chemically abrupt interfaces formed between polar and nonpolar perovskite oxides provide an ideal platform for examining the purely electronic reconstruction known as the polar catastrophe and the emergence of mobile or bound charges at the interface. The appearance of mobile charges induced by the polar catastrophe is already established in the $LaAlO_3/SrTiO_3$ heterojunctions. Although not experimentally verified, the polar catastrophe can also lead to the emergence of spontaneous polarization. We report that thin films of originally nonpolar $LaFeO_3$ grown on $SrTiO_3$ are converted to polar as a consequence of the polar catastrophe. The induced spontaneous polarization evokes photovoltaic properties distinct from conventional *p-n* junctions, such as a switching of the photocurrent direction by changing the interfacial atomic sequence. The control of the bulk polarization by engineering the interface demonstrated here will expand the possibilities for designing and realizing new polar materials with photovoltaic functions.

DOI: 10.1103/PhysRevLett.116.156801

Emergence of mobile and/or bound charges at an interface with a discontinuous valence state, or the so-called polar discontinuity, has been one of the central research topics in recent material science [1–4]. The idea of charge generation stemming from the polar discontinuity was first examined in semiconductor heterojunctions such as Ge/GaAs(110) [5]. However, atomic interdiffusion is more favored than purely electronic reconstruction, and the idea was not verified in these junctions. The revival of interest in the polar interface was brought about by the discovery of high-mobility two-dimensional (2D) interface conduction in the $LaAlO_3$ (LAO)/$SrTiO_3$ (STO) heterojunction [1]. Because of the structural robustness and the small atomic diffusibility in perovskite oxides, their interfaces can be kept abrupt even in the polar junction. Therefore, such interfaces offer an ideal platform to see pure electronic reconstructions and accompanying phenomena distinct from conventional semiconductor interfaces such as superconductivity [6] and magnetism [7].

The emergence of 2D conduction in the LAO/STO junction is generally explained by the so-called polar catastrophe scenario as follows [8,9]. The presence of the polar discontinuity at the interface causes the high density bound charges at the interface (0.5 e/unit cell, corresponding to 53 $\mu C/cm^2$) [9,10]. Because these bound charges evoke a linear divergence of the electrostatic potential with increasing LAO thickness, the junction reduces the energy cost above a certain critical thickness by either collecting electrons to the interface through charge transfer [8] or by creating oxygen vacancies and/or other defects on the LAO surface [11–13]. Since the polar catastrophe is a process of charge redistribution necessary to screen the interfacial bound charges, the polar catastrophe can also lead to the displacement of ions or electronic wave functions, thus creating spontaneous electric polarization, even without collecting mobile charges. Although the emergence of spontaneous polarization has been theoretically predicted [14,15], its influence on the junction property is masked by the existence of the mobile charges and therefore is hard to be detected in the LAO/STO junction.

Here, we explore oxide heterojunctions in which spontaneous polarization plays a dominant role in the charge screening. The target materials are trivalent transition-metal-oxide insulators, which do not form a conductive interface with STO even though the interface has a polar discontinuity [16]. Among them, $LaFeO_3$ (LFO) is one of the most suitable materials, which is known as a centrosymmetric Mott insulator with an optical gap (2.2 eV) in the visible-light region [17]. It has a high resistivity compared to other Mott insulators due to the closed-shell structure in the up-spin band of the Fe^{3+} state [18]. Furthermore, it shows an instability toward the polar state under epitaxial strain [19]. Thus, the LFO/STO junction lends itself as a attractive model system to examine interface-induced spontaneous polarization.

We deposited 30-nm-thick LFO films on 0.5-mm-thick STO and $SrTi_{0.9998}Nb_{0.0002}O_3$ (Nb:STO) substrates with controlled TiO_2 and SrO terminations as illustrated in Fig. 1(a) [20]. Figure 1(b) shows the atomic structure and elemental distributions near the LFO/STO interfaces imaged by a scanning transmission electron microscope

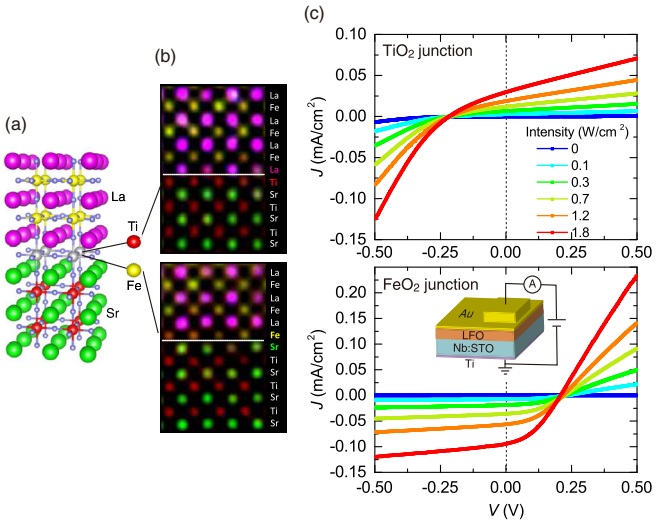

FIG. 1. (a) A schematic of the elemental stacking in the LFO/STO junctions. The interfacial atomic layers were controlled and were either TiO_2 or FeO_2 layers. (b) Elemental distribution mappings for a TiO_2 junction (upper panel) and a FeO_2 junction (lower panel) taken with a STEM, where atomic resolution energy-dispersive x-ray spectroscopy images are superimposed on high-angle annular dark images. Line profiles of the elemental distribution are shown in the Supplemental Material [20]. (c) Current density (J)–voltage (V) properties of the LFO/Nb:STO junctions upon shinning laser light. The wavelength of the laser is 473 nm. The positive direction of the applied voltage is defined by the schematics illustrated in the inset.

(STEM) and energy dispersive x-ray spectroscopy (EDX). The image verifies that the elemental sequence is constructed as we designed. The broadening of the distribution estimated from the line profiles of the STEM-EDX intensities remains at most 2 unit cell from the interface [20], indicating that the interface is abrupt enough to classify the interfacial atomic sequence into two definite types and that the effect of interfacial disorder is negligible. Hereafter, we denote the junctions formed on the TiO_2- and SrO-terminated STO surfaces as the "TiO_2 junction" and the "FeO_2 junction" according to the interfacial transition-metal layer, respectively. We confirmed that there is no detectable lateral conductivity in those LFO/STO junctions, irrespective of the interface terminations.

The current density (J)–voltage (V) characteristics of the junctions measured under photoillumination are shown in Fig. 1(c). Here, we shined laser light with a wavelength of 473 nm ($\hbar\omega = 2.6$ eV), which is absorbed only by LFO. The most prominent feature is that the sign of both the short-circuit photocurrent and the rectifying polarity is reversed by altering the interface termination. Similar switching behavior in the photovoltaic properties has been reported upon ferroelectric polarization reversals in many ferroelectrics [28–30]. Following this analogy, we expect that our LFO films have an electric polarization, whose direction is inverted upon altering the interfacial atomic sequence. As discussed later, the polarization direction is fixed by the interfacial atomic sequence and cannot be reversed by electric fields.

To directly see the existence of the electric polarization, we employed piezoresponse force microscopy (PFM) to study a sample that is fabricated so that it has both TiO_2 and FeO_2 junctions within the same substrate as shown in Fig. 2(a) [20]. Thus, the opposite polarization directions between the two junctions can be clearly visualized within one experimental run. The phase image of the PFM shown in Fig. 2(b) exhibits a clear contrast at the boundary with a phase shift of nearly 180°, indicating that the LFO films have electric polarization components pointing normal to the film surface and that their directions are opposite in the two regions. Although this provides clear evidence for the presence of an electric polarization P, it still remains unclear whether the polarization is induced by the dielectric response P_d, or is a spontaneous polarization P_s existing even without the internal electric field.

Electron holography can directly quantify the spatial distribution of the electrostatic potential and accordingly the built-in internal electric field in a specimen [20]. By employing this technique, we examined the possible origin of P. Figure 3(a) shows the mappings of the electrostatic potentials for an electron, which are derived from the phase shift of the object waves. The electrostatic potential is almost uniform in the in-plane direction in both junctions. We now examine in detail the electrostatic potential and show in Fig. 3(b) two examples of the electrostatic potential obtained along the dashed lines in Fig. 3(a). First, the large potential drop near the interface is merely due to the difference in the mean inner potential between LFO and STO and we can thus ignore it in the following discussions. Second, the electrostatic potential has opposite slopes in the two LFO junctions. The electron potential in LFO grows (falls) from the interface to the surface in the TiO_2 (FeO_2) junction with an electric field E of -58 kV/cm ($+81$ kV/cm) as illustrated in Fig. 3(c), where a positive E corresponds to the field pointing from the surface to the bottom of LFO following the definition of the current

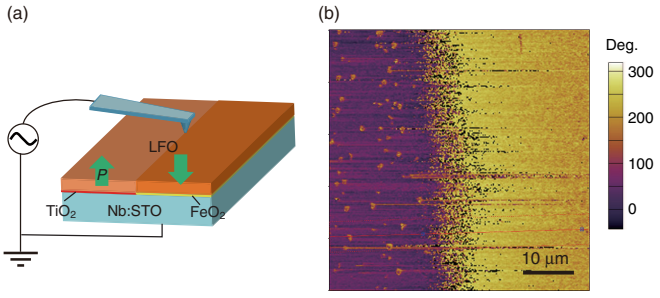

FIG. 2. (a) A schematic of the piezoresponse force microscope observation for a LFO film grown on a Nb doped STO substrate having both TiO_2 and SrO surface terminated regions on the surface. (b) Observation of artificially tailored polarization domains by the piezoresponse force microscope as a phase image. The boundary of the opposite polarization domains is coincident with that of the interface termination.

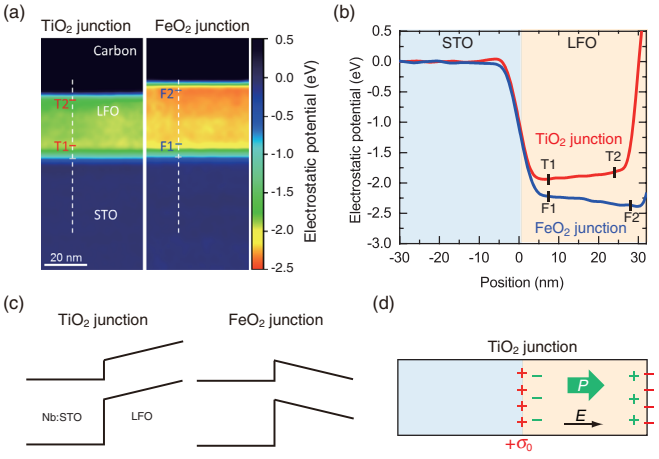

FIG. 3. (a) Mappings of the electrostatic potentials derived from electron holography for two differently interface terminated LFO/STO junctions. Here, we show the potentials for an electron. (b) Line profiles of the potentials along the dashed lines in (a). (c) Possible band structure in the LFO/STO junctions deduced from the potential profiles in (b) and capacitance measurements [20]. (d) A model for electrostatic conditions in a TiO_2 junction. σ_0 denotes the bound charges stemming from the polar discontinuity between LFO and STO. P is an electric polarization induced in LFO to partially screen σ_0. E is a built-in electric field originating from the remnant interface charges $(\sigma_0 - P)$.

direction. The direction of E is consistent with the expected sign of the interface bound charge [31]. Third, no appreciable potential variation can be seen in STO, which is consistent with no detectable lateral conductivity in the LFO/STO junction. This is in contrast to the downward bending in the case of TiO_2-terminated LAO/STO that accumulates electrons.

Having clarified the magnitude of the built-in electric field, we now analyze the electrostatic conditions in LFO/Nb:STO junctions. The polar discontinuity entails a bound charge of $+0.5\ e$/unit cell ($53\ \mu C/cm^2$) denoted as σ_0 in Fig. 3(d). We assume that the screening of σ_0 is realized only by the induced polarization (P) in LFO. Then, the potential slope or the built-in electric field (E) observed by electron holography originates from the interfacial remnant charge $(\sigma_0 - P)$ given by

$$\sigma_0 - P = \varepsilon_0 E, \tag{1}$$

where ε_0 is the vacuum permittivity. P is the sum of the dielectric polarization (P_d) and the spontaneous one (P_s), i.e., $P = P_d + P_s$, and P_d is given by

$$P_d = \chi E = \varepsilon_0 \varepsilon_r E, \tag{2}$$

where ε_r stands for the relative dielectric constant of LFO, which is derived to be 35 from a capacitance measurement [20]. Using $E = -58$ kV/cm in the TiO_2 junction, we obtain $P_d = 0.17\ \mu C/cm^2$. This value of P_d is far smaller than σ_0, implying that a large part of the screening charge relies on P_s in our model. Note that, in reality, a part of the screening charge is supplied from the mobile carriers in Nb:STO as revealed by the capacitance measurements [20]. However, both the sign reversal in the polarity of the photovoltaic property and the phase shift of 180° in the PFM observation indicate that a large part of the screening charge comes from P induced in the LFO films.

The existence of the large P_s deduced from the above analysis is justified by the anomalous photovoltaic properties. The direction of the photocurrent should be aligned to the electric field in conventional dielectrics. However, the experimentally observed short-circuit photocurrent [Fig. 1(c)] flows opposite to the direction of the built-in electric field [Fig. 4(a)], and is also opposite to that reported for the LAO/STO junction where the spontaneous polarization is negligibly small after mobile carriers are induced by the polar catastrophe [32]. This means that the photocurrent in our junctions originates from a different mechanism, likely being associated with P_s. Here, we introduce the concept of a shift current J_{shift} as a possible origin of the photocurrent in our junctions. It is known that single-domain noncentrosymmetric materials can generate a dc current under uniform photoillumination, namely, the bulk photovoltaic effect [33]. A main origin of the bulk photovoltaic effect that has been recently proven is the shift current [34–36]. The shift current arises from the quantum mechanical displacement of the photoinduced carriers relative to the initial state in real space due to the asymmetric electronic potential in inversion-broken materials as depicted in Fig. 4(a). The shift current flows to the direction of the so-called shift vector given by the difference in the Berry connections between the initial and excited states [35,36]. Therefore, the shift current direction depends strongly on the relevant band structure rather than the macroscopic electric field. We consider that the shift current and drift current J_{drift} are coexisiting in our junctions, and the shift current is the origin of the photocurrent flowing opposite to E.

The coexistence of J_{shift} and J_{drift} is evidenced in the spectral distribution of the short-circuit photocurrent J_{SC}, the so-called photocurrent action spectra. As shown in Fig. 4(b), the sign of J_{SC} reverses in the TiO_2 junction with a LFO thickness of 20 nm, from negative to positive at a photon energy of 3.2 eV. The negative (positive) J_{SC} indicates a dominating J_{drift} (J_{shift}). The sign change occurs because of the enlargement of J_{shift} at higher photon energies. Such a sign reversal is not observed in the junctions with $t = 13$ nm and 30 nm in the entire photon energy range, but these two junctions have an opposite J_{SC}: in the former (latter), the sign is negative (positive). We examined the position dependence of the photocurrent action spectra in an array of devices [20]. The spectra are reproducible and independent of the device position, implying that the anomalous sign change in the photocurrent is not induced by local defects [25].

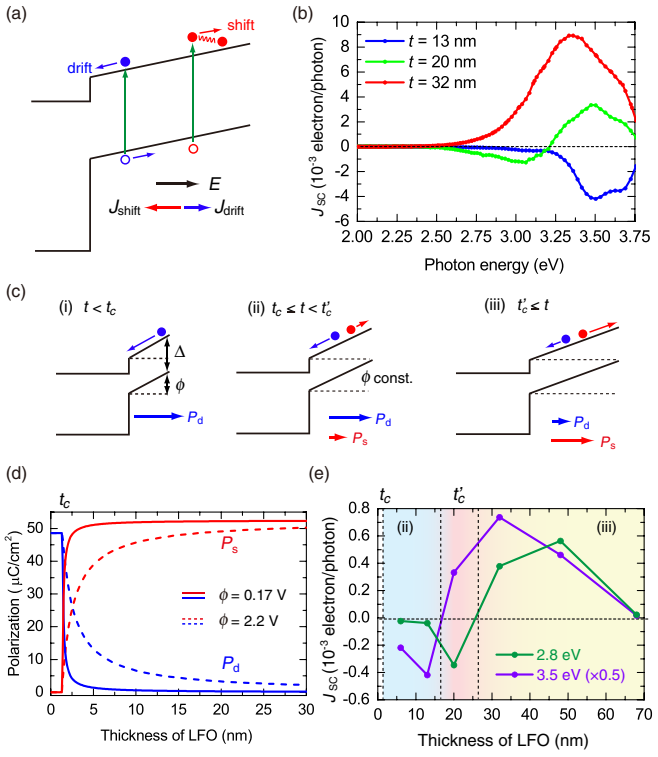

FIG. 4. (a) Schematic of two possible origins of the photocurrent in the LFO/STO junction. The shift current (J_{shift}) is induced by spontaneous polarization while the drift current (J_{drift}) is induced by the internal electric field. (b) Photocurrent action spectra for TiO_2 junctions with different LFO thicknesses. (c) Band structures and photocurrent generation in the LFO/STO junctions in three thickness ranges. Δ and ϕ stand for the band gap of LFO and the potential elevation, respectively. Case (i): the slope of the electrostatic potential is constant and the origin of the photocurrent is J_{drift} only. Case (ii): when $t > t_c$, ϕ is constant and J_{drift} and J_{shift} coexist. Case (iii): at $t = t_c' > t_c$, J_{shift} becomes more dominant than J_{drift}. (d) Calculated thickness dependence of the spontaneous polarization (P_s) and dielectric polarization (P_d) on the basis of the band structure. The solid (dashed) lines correspond to the case of $\phi = 0.17$ (2.2) eV. (e) Magnitude of the photocurrent as a function of the thickness of LFO in TiO_2 junctions measured at 2.8 and 3.5 eV.

Now we discuss an evolution of the polarization and accordingly the change in the photocurrent with thickness on the basis of the polar catastrophe model. There are two characteristic thicknesses t_c and t_c'. t_c is the thickness at which the polar catastrophe sets on and t_c' is the thickness at which J_{SC} reverses sign. We consider the mechanisms of photocurrent generation in the following three thickness ranges: (i) $t < t_c$, (ii) $t_c \le t < t_c'$, and (iii) $t_c' \le t$, as shown in Fig. 4(c). In case (i), the spontaneous polarization is absent ($P_s = 0$) and most of σ_0 is screened by the dielectric response associated with the large thickness-independent E. Equations (1) and (2) give $E = \sigma_0/\varepsilon_0(1+\varepsilon_r)$, and E is estimated to be -17 MV/cm in LFO. Because of the large E, J_{drift} is dominant in this thickness range, resulting in the same direction in between E and J_{SC}. When the potential elevation ϕ reaches the band gap of LFO ($\Delta = 2.2$ eV), the polar catastrophe occurs and triggers the emergence of P_s. We define this thickness as t_c, given by $\varepsilon_0(1+\varepsilon_r)\Delta/\sigma_0$, which is estimated to be 1.4 nm (~3 u.c.) in the LFO/STO junction. For $t > t_c$, E decreases in inverse proportion to t because ϕ is limited by Δ. In contrast, P_s grows with t to compensate for the reduced dielectric response. Since $J_{drift} \propto E$ and J_{shift} has a positive correlation with P_s, J_{drift} (J_{shift}) decreases (increases) with t, implying that J_{drift} and J_{shift} cross at some thickness, which we define as t_c'. In case (ii), J_{drift} is still larger than J_{shift} and hence J_{SC} and E point in the same direction, which is the case for the junction with $t = 13$ nm. In case (iii), J_{shift} overcomes J_{drift} and hence J_{SC} flows opposite to E as observed for the junction with $t = 32$ nm. Hence, the junction with $t = 20$ nm will be located very close to the critical thickness t_c'.

Figure 4(d) shows the dependence of P_s and P_d on t calculated on the basis of the polar catastrophe model. The curves are plotted for $\phi = 2.2$ eV and 0.17 eV, which are the upper limit estimated from the band gap of LFO and the lower limit estimated from electron holography, respectively. Figure 4(e) shows the thickness dependence of the photocurrent at 2.8 and 3.5 eV obtained from the action spectra. The sign is negative in the thinner junctions due to the dominant J_{drift} and switches to positive in the thicker junctions driven by the enhanced J_{shift}. The sign reversal occurs between 17 and 25 nm depending on the photon energy, implying that t_c' locates in this thickness range. The photocurrent of the thickest film of nearly 70 nm is quite small. This is probably because the typical length of the shift vector is 10–100 nm and the photocurrent reduces when the film thickness exceeds this length [37]. Thus, the model calculation of P_s and P_d shown in Fig. 4(d) can qualitatively explain the thickness dependence of the photocurrent, although the relation between J_{shift} and the electric polarization is complicated and a quantitative estimation of J_{shift} is currently impossible.

We again emphasize that the dominant screening mechanism of the polar discontinuity in the LFO/STO junction is spontaneous polarization, unlike the mobile charges in LAO/STO. The reason for the difference between the LFO/STO and LAO/STO junctions may be as follows. According to a first-principles calculation, $R\mathrm{FeO_3}$ (R stand for rare-earth elements) can show a spontaneous polarization of over 100 μC/cm^2 if a 7% compressive strain is applied [19]. Because the strain in our LFO film is only 1%, the epitaxial strain alone is unlikely to be a sufficient story to induce the polar state. Yet, the instability toward the polar state in LFO will assist the emergence of spontaneous polarization.

In summary, we have revealed the emergence of spontaneous polarization in $\mathrm{LaFeO_3/SrTiO_3}$ heterojunctions. The existence of an electric polarization was verified by piezoresponse force microscopy. Furthermore, electron holography has revealed that the spontaneous polarization dominates the electric polarization. The polarization

direction can be switched by choice of the interfacial atomic sequence. The emergent spontaneous polarization induces anomalous photovoltaic properties in the junctions, such as a sign reversal in the photocurrent depending on the interfacial atomic sequence and the excitation photon energy. The present demonstration implies that control of the bulk polarization can be achieved by engineering the interface. Recently, visible-light-absorbable polar oxides have been widely explored and suggested to be efficient photovoltaic materials [38–40]. Our present results offer a feasible way of realizing new photovoltaic materials from narrow-gap and nonpolar ones by engineering the hetero-interfaces of oxides.

We acknowledge H. Y. Hwang, A. Tsukazaki, N. Ogawa, and D. Maryenko for useful discussions and Y. Ohtsu and T. Sato for TEM observations. This work was partly supported by the Japan Society for the Promotion of Science (JSPS) through its Funding Program for World-Leading Innovative R&D on Science and Technology (FIRST Program), and by CREST from the Japan Science and Technology Agency (JST). It was also supported by a Grant-in-Aid for Young Scientists (A) (15H05426) and Grant-in-Aid for Scientific Research (24226002) from the MEXT of Japan.

*masao.nakamura@riken.jp
†Present address: Research and Development Group, Hitachi, Ltd., Hatoyama, Saitama 350-0395, Japan.
‡Present address: Department of Materials Science and Engineering, Dong-A University, Busan 604-714, Republic of Korea.

[1] A. Ohtomo and H. Y. Hwang, Nature (London) **427**, 423 (2004).
[2] J. Mannhart and D. G. Schlom, Science **327**, 1607 (2010).
[3] R. Pentcheva and W. E. Pickett, J. Phys. Condens. Matter **22**, 043001 (2010).
[4] H. Y. Hwang, Y. Iwasa, M. Kawasaki, B. Keimer, N. Nagaosa, and Y. Tokura, Nat. Mater. **11**, 103 (2012).
[5] W. A. Harrison, E. A. Kraut, J. R. Waldrop, and R. W. Grant, Phys. Rev. B **18**, 4402 (1978).
[6] N. Reyren *et al.*, Science **317**, 1196 (2007).
[7] A. Brinkman, M. Huijben, M. van Zalk, J. Huijben, U. Zeitler, J. C. Maan, W. G. van der Wiel, G. Rijnders, D. H. A. Blank, and H. Hilgenkamp, Nat. Mater. **6**, 493 (2007).
[8] N. Nakagawa, H. Y. Hwang, and D. A. Muller, Nat. Mater. **5**, 204 (2006).
[9] N. C. Bristowe, P. Ghosez, P. B. Littlewood, and E. Artacho, J. Phys. Condens. Matter **26**, 143201 (2014).
[10] M. Stengel and D. Vanderbilt, Phys. Rev. B **80**, 241103 (2009).
[11] C. Cen, S. Thiel, G. Hammerl, C. W. Schneider, K. E. Andersen, C. S. Hellberg, J. Mannhart, and J. Levy, Nat. Mater. **7**, 298 (2008).
[12] Y. Li, S. N. Phattalung, S. Limpijumnong, J. Kim, and J. Yu, Phys. Rev. B **84**, 245307 (2011).
[13] L. Yu and A. Zunger, Nat. Commun. **5**, 5118 (2014).
[14] N. C. Bristowe, E. Artacho, and P. B. Littlewood, Phys. Rev. B **80**, 045425 (2009).
[15] R. Pentcheva and W. E. Pickett, Phys. Rev. Lett. **102**, 107602 (2009).
[16] S. A. Chambers, L. Qiao, T. C. Droubay, T. C. Kaspar, B. W. Arey, and P. V. Sushko, Phys. Rev. Lett. **107**, 206802 (2011).
[17] M. Imada, A. Fujimori, and Y. Tokura, Rev. Mod. Phys. **70**, 1039 (1998).
[18] T. Arima, Y. Tokura, and J. B. Torrance, Phys. Rev. B **48**, 17006 (1993).
[19] H. J. Zhao, Y. Yang, W. Ren, A.-J. Mao, X. M. Chen, and L. Bellaiche, J. Phys. Condens. Matter **26**, 472201 (2014).
[20] See Supplemental Material at http://link.aps.org/supplemental/10.1103/PhysRevLett.116.156801, for details on the sample fabrication and measurements, which includes Refs. [21–27].
[21] M. Kawasaki, K. Takahashi, T. Maeda, R. Tsuchiya, M. Shinohara, O. Ishiyama, T. Yonezawa, M. Yoshimoto, and H. Koinuma, Science **266**, 1540 (1994).
[22] G. Kothleitner, M. J. Neish, N. R. Lugg, S. D. Findlay, W. Grogger, F. Hofer, and L. J. Allen, Phys. Rev. Lett. **112**, 085501 (2014).
[23] M. Nakamura, A. Sawa, J. Fujioka, M. Kawasaki, and Y. Tokura, Phys. Rev. B **82**, 201101(R) (2010).
[24] T. Tanigaki, Y. Inada, S. Aizawa, T. Suzuki, H. S. Park, T. Matsuda, A. Taniyama, D. Shindo, and A. Tonomura, Appl. Phys. Lett. **101**, 043101 (2012).
[25] L. Pintilie, V. Stancu, E. Vasile, and I. Pintili, J. Appl. Phys. **107**, 114111 (2010).
[26] W. Siemons, G. Koster, H. Yamamoto, W. A. Harrison, G. Lucovsky, T. H. Geballe, D. H. A. Blank, and M. R. Beasley, Phys. Rev. Lett. **98**, 196802 (2007).
[27] G. Herranz, M. Basletić, M. Bibes, C. Carrétéro, E. Tafra, E. Jacquet, K. Bouzehouane, C. Deranlot, A. Hamzić, J.-M. Broto, A. Barthélémy, and A. Fert, Phys. Rev. Lett. **98**, 216803 (2007).
[28] T. Choi, S. Lee, Y. J. Choi, V. Kiryukhin, and S.-W. Cheong, Science **324**, 63 (2009).
[29] C. J. Won, Y. A. Park, K. D. Lee, H. Y. Ryu, and N. Hur, J. Appl. Phys. **109**, 084108 (2011).
[30] Y. Yuan, T. J. Reece, P. Sharma, S. Poddar, S. Ducharme, A. Gruverman, Y. Yang, and J. Huang, Nat. Mater. **10**, 296 (2011).
[31] G. Singh-Bhalla, C. Bell, J. Ravichandran, W. Siemons, Y. Hikita, S. Salahuddin, A. F. Hebard, H. Y. Hwang, and R. Ramesh, Nat. Phys. **7**, 80 (2011).
[32] H. Liang *et al.*, Sci. Rep. **3**, 1975 (2013).
[33] B. I. Sturman and V. M. Fridkin, *The Photovoltaic and Photorefractive Effects in Noncentrosymmetric Materials.* (Gordon and Breach Science Publishers, New York, 1992).
[34] R. von Baltz and W. Kraut, Phys. Rev. B **23**, 5590 (1981).
[35] S. M. Young and A. M. Rappe, Phys. Rev. Lett. **109**, 116601 (2012).
[36] T. Moritomo and N. Nagaosa, arXiv:1510.08112.
[37] A. Zenkevich, Yu. Matveyev, K. Maksimova, R. Gaynutdinov, A. Tolstikhina, and V. Fridkin, Phys. Rev. B **90**, 161409(R) (2014).
[38] S. Y. Yang *et al.*, Appl. Phys. Lett. **95**, 062909 (2009).
[39] I. Grinberg *et al.*, Nature (London) **503**, 509 (2013).
[40] R. Nechache, C. Harnagea, S. Li, L. Cardenas, W. Huang, J. Chakrabartty, and F. Rosei, Nat. Photonics **9**, 61 (2015).